*Biochimica et Biophysica Acta* 861 (1986) 471–479
Elsevier



BBA 73320

# Delayed activation of calcium pump during transient increases in cellular $Ca^{2+}$ concentration and $K^+$ conductance in hyperpolarizing human red cells

Ole Scharff and Birthe Foder

*Department of Clinical Physiology and Nuclear Medicine, Rigshospitalet, Blegdamsvej 9, DK-2100 Copenhagen (Denmark)*

(Received 10 June 1986)

Key words: $Ca^{2+}$ transport; $Ca^{2+}$ transient; $K^+$ channel; Hysteresis; Oscillation; (Human erythrocyte)

**The net $Ca^{2+}$ influx was increased in human red cells in suspension by adding moderate concentrations of the $Ca^{2+}$ ionophore A23187, and due to the increased cellular $Ca^{2+}$ concentration ($[Ca]_i$) the $K^+$ channels opened (the 'Gardos effect'). At low $K^+$ concentration and with the protonophore CCCP in the buffer-free medium the cells hyperpolarized and the extracellular pH ($pH_0$) increased, enhancing the A23187-mediated net $Ca^{2+}$ influx. This elicited a prolonged response, viz. a primary transient increase of $pH_0$ and $[Ca]_i$ followed by one or more spontaneous $pH_0$ and $[Ca]_i$ transients. We explored the pump-mediated $Ca^{2+}$ efflux by blocking the A23187-mediated $Ca^{2+}$ flux with $CoCl_2$ at appropriate times during the prolonged response. The $Ca^{2+}$ pumping was higher during the descendent than during the ascendent phase of the primary transient at equal values of $[Ca]_i$. The data were anlyzed using a mathematical model that accounts for the prolonged oscillatory response, including $pH_0$ and $[Ca]_i$. In conclusion, the activation of the $Ca^{2+}$ pump is delayed due to slow binding of cellular calmodulin, which is a hysteretic response to a rapid increase of the cellular $Ca^{2+}$ concentration. This mechanism may be important for generation and execution of transient signals in other types of cell.**

## Introduction

The calcium pump in human red cells is located in the plasma membrane and has the ability to transport calcium ions from the cytoplasm to the extracellular medium against an electrochemical gradient utilizing ATP as the energy source (for recent reviews see Refs. 1 and 2). The calcium pump exhibits maximum activity when binding calmodulin [3–6], and the binding constants and the rate of binding are strongly dependent on the $Ca^{2+}$ concentration, as suggested from $Ca^{2+}$-ATPase experiments [7]. The cytoplasmic concentration of ionized calcium in human red cells seems to be in the range $10^{-8}$ to $10^{-7}$ M [1,8], and at that concentration calmodulin should be dissociated from the calcium pump [9].

In intact human red cells suspended in blood plasma the steady-state flux of $Ca^{2+}$ over the plasma membrane is about 50 $\mu$mol/h per l cells [1,8] or about 0.3% of the maximum activity of the calcium pump. The $Ca^{2+}$ influx can be increased by adding the $Ca^{2+}$-transporting ionophore A23187 to a suspension of the red cells, and at an appropriate low concentration of A23187 the cells respond with a transient increase of the cellular concentration of calcium [9,10].

Based on experiments with $Ca^{2+}$/calmodulin activation of membrane-bound $Ca^{2+}$-ATPase we have suggested that the occurrence of the calcium

Abbreviations: CCCP, carbonyl cyanide *m*-chlorophenylhydrazone.

Correspondence address: Dr. O. Scharff, Department of Clinical Physiology and Nuclear Medicine, Rigshospitalet, Blegdamsvej 9, DK-2100 Copenhagen, Denmark.

transients described above is conditional on a delayed activation of the calcium pump [9].

The delay in activation of the calcium pump is expected if it is assumed that $Ca^{2+}$, calmodulin and the pump ATPase are constituent parts of a hysteretic enzyme system that responds slowly to a rapid increase of the concentration of one ligand, in this case $Ca^{2+}$, as shown below in a mathematical model.

In an attempt to demonstrate directly the delayed calcium pump activation in intact human red cells we have taken advantage of two recent techniques, one giving a pH-dependent acceleration of the A23187-mediated $Ca^{2+}$ influx and rapid increase of cellular $Ca^{2+}$ concentration [11,12], another making it possible to block rapidly the A23187-mediated $Ca^{2+}$ flux without affecting the pump flux [13].

## Materials and Methods

Radioactive calcium ($^{45}CaCl_2$) was purchased from Amersham (0.6–0.9 GBq/mg Ca) and diluted with $CaCl_2$ solution before use. Ionophore A23187 (Calbiochem) was stored as a stock solution (1.55 mM) in ethanol/acetone (9 : 1, v/v) at −20°C and diluted (1 : 10) with ethanol before use. CCCP (Sigma) was administered as ethanol solution (20 mM). All other chemicals were from Merck (pro analysis).

Human blood from healthy donors was collected in citrate-phosphate-dextrose solution, stored at 4°C, and used within 1 day.

*Transport experiments with glucose-fed cells.* Immediately before use the blood plasma and buffy coat were removed by centrifugation (20000 × *g* for 1 min) and the red cells were washed at room temperature three times in the incubation medium containing (mM): NaCl (155), KCl (1), $MgCl_2$ (0.15), and glucose (5). The washed cells were resuspended at 37°C in the incubation medium including, in addition, CCCP (0.02) and $^{45}CaCl_2$ to a final concentration of about 10 μM (60–90 MBq/mg $Ca^{2+}$), the pH was adjusted with NaOH (155), and the suspension was vigorously stirred during the mixing and the experimental period. The total volume of cell suspension was 8 ml and the cell volume fraction was about 4%. The experiment was started by addition of A23187 solution.

For the determination of calcium pump flux the A23187-mediated $Ca^{2+}$ flux was blocked by the addition of $CoCl_2$ solution to a final concentration of 0.25 mM in the medium (cf. Results).

The addition of the protonophore CCCP made it possible to follow changes of the membrane potential by measuring the extracellular pH (see Results and Ref. 11). Extracellular pH was monitored continuously during the experiment by a glass electrode (G202C) and a calomel electrode (K401) immersed in the cell suspension and connected via a pH-meter (TTT1c, all Radiometer) to a recorder. At the end of the experiment the cells were haemolysed by the addition of 100 μl Triton X-100 (10%, v/v), which allowed the determination of the cellular pH due to the lack of other buffers in the medium.

*Transport experiments with ATP-depleted cells.* To the stored whole blood were added (mM, final concentration): NaCl (80), KCl (75), $MgCl_2$ (0.15), inosine (10), iodoacetamide (6), and sodium glycolate (15), to a final cell volume fraction of 10%, and the cell suspension was incubated at 37°C for 2.5 h. Then the red cells were isolated and washed three times in the incubation medium chosen. This treatment reduced the ATP concentration of the washed cells to 1 μmol/l cells [14]. Incubation and start of the experiment were as above except for the omission of glucose from the medium.

The experiments with ATP-depleted cells were performed in order to determine the A23187-mediated net influx of $Ca^{2+}$ into the red cells. The flux parameters were determined as previously [14] in the presence of either low (1 mM) or high (75–100 mM) extracellular concentration of potassium chloride, leading to parameters for A23187-mediated $Ca^{2+}$ flux in hyperpolarized and non-hyperpolarized cells, respectively.

*Determination of cellular calcium concentration.* This method is modified from Lew and Brown [15] and has been described previously in detail [9]. With intervals of at least 7.5 s, samples (200 μl) were transferred from the incubating cell suspension to centrifuge tubes containing a stop buffer and dibutylphthalate oil (density 1.042–1.045). Subsequently, the cell pellet was isolated below the oil layer by centrifugation (20000 × *g* for 20 s), and the pellet was processed for scintillation counting of $^{45}Ca$ in a Packard Tricarb (3255)

counter. The cellular calcium concentration ($\mu$mol/l packed cells) was calculated from the measured cellular and total radioactivities and from the total concentration of calcium in the cell suspension, using the haematocrit values determined during the experiment.

$Ca^{2+}$-ATPase assay and determination of calcium were performed as previously [16]. The extracellular $Ca^{2+}$ concentration of the medium was monitored by atomic absorption measurements of separate samples of cell suspension centrifuged before the addition of A23187.

## Results

*Calcium uptake caused by A23187*

The addition of the calcium ionophore A23187 to a suspension of glucose-fed human red cells in the presence of $^{45}Ca^{2+}$ revealed a transient increase of the cellular calcium concentration. A typical experiment is shown in Fig. 1.

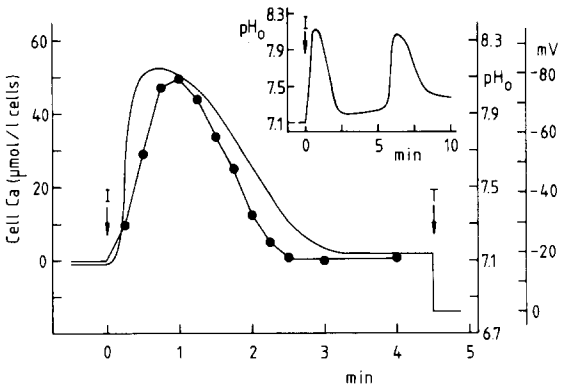


Fig. 1. Changes of extracellular pH and cellular calcium concentration dependent on time after addition of ionophore A23187. Washed human red cells (glucose-fed) were suspended in (mM): NaCl (155), KCl (1), $MgCl_2$ (0.15), glucose (5), pH 7.08, 37°C (see Methods). $^{45}CaCl_2$ was added to the cell suspension to a total extracellular concentration of 10 $\mu$M. Initial cell volume fraction was 4.2%. A23187 ('I') was added at zero time (9.7 $\mu$mol/l cells). Triton X-100 (to about 0.1%) was added at 4.5 min ('T') in order to haemolyse the cells, which showed the cellular pH 6.82. The membrane potential is the pH difference multiplied by 61.5 mV. pH and potential (continuous curve), cell Ca (●). Inset, changes in extracellular pH showing a spontaneous second transient caused by a single A23187 addition at zero time. A spontaneous third transient (not shown) appeared 20 min after A23187 addition. Conditions above.

The calcium transient was accompanied by a transient increase of the potassium conductance due to a $Ca^{2+}$-mediated opening of the potassium channels, as described earlier [11,17]. In the case of an extracellular potassium concentration well below the equilibrium value, which was between 75 and 100 mM, the increased potassium conductance led to a hyperpolarisation of the membrane. The protonophore CCCP was added to the cell suspension in order to facilitate the transport of protons between the intracellular buffers (primarily haemoglobin) and the buffer-free extracellular medium. Thereby the measurement of extracellular pH can reveal changes in the membrane potential, and it appears from Fig. 1 that the membrane potential changed transiently from $-16$ to $-82$ mV.

The extracellular pH increased faster than the cellular $Ca^{2+}$ concentration. During the first 30 s after the A23187 addition the pH increment and the $Ca^{2+}$ concentration reached (mean $\pm$ S.E., $n$ = 8) $85 \pm 6\%$ and $50 \pm 7\%$, respectively, of their maximum values. This indicates that the opening of the potassium channels, and consequently the hyperpolarisation, was initiated at low cellular $Ca^{2+}$ concentrations (Fig.1). The subsequent decreases of extracellular pH and cellular $Ca^{2+}$ concentration, however, occurred either simultaneously or in reverse order.

The A23187-mediated $Ca^{2+}$ flux depends strongly on the proton gradient across the membrane [12]. During the transient increase of extracellular pH in our experiments the A23187-mediated maximum $Ca^{2+}$ influx first increased (5–15-fold) and then decreased due to the change in the extracellular pH.

The advantage of using the increase of extracellular pH in order to obtain a rapid increase of the intracellular calcium concentration instead of employing a higher A23187 concentration was the following: after obtaining the maximum $Ca^{2+}$ flux at the top of the pH transient the flux decreased again, which allowed the calcium pump to adjust to a lower steady-state level of cellular calcium concentration at the end of the transient (see Fig. 1) than would be possible at the higher $Ca^{2+}$ fluxes mediated by high A23187 concentrations (not shown). The low steady-state level at the end of the transient was necessary in order to

compare calcium pump fluxes at low cellular calcium concentrations during the ascendent and the descendent phases of the transient (cf. later).

The disadvantage of using low extracellular potassium concentrations in these experiments was that the cells lost potassium chloride and water, i.e. the cells shrank during the calcium transient. Typically, the cell volume decreased about 20% during the first transient.

In several experiments the first transient increase of extracellular pH was followed by spontaneous pH transients (Fig. 1, insert) similar to the oscillations described previously [11,18,19], and these spontaneous pH transients were accompanied by transient changes in the cellular $Ca^{2+}$ concentration similar to those found in the first transient.

*Effect of $CoCl_2$ on $Ca^{2+}$ flux*

The increased $Ca^{2+}$ influx into human red cells caused by addition of the ionophore A23187 to the cell suspension can be blocked by the addition of either cobalt chloride or albumin, apparently without significant inhibition of the calcium pump [13]. Some effects of cobalt chloride are demonstrated in Fig. 2.

Addition of $CoCl_2$ before the addition of A23187 totally prevented the uptake of $^{45}CaCl_2$ from the extracellular medium into cells depleted of ATP during the first 3–4 min and the cobalt chloride still inhibited the $Ca^{2+}$ influx up to 15 min after the addition of ionophore (Fig. 2, inset).

Cobalt chloride also inhibited the A23187-mediated $Ca^{2+}$ flux when added to red cells already loaded with $^{45}CaCl_2$ by preincubation in the presence of A23187 (Fig. 2). Glucose-fed cells and ATP-depleted cells accumulated $Ca^{2+}$ at 1°C at nearly the same rate but when transferred to 37°C the fed cells (containing about 1 mmol ATP/l cells), in contrast to the depleted cells (containing 1 μmol ATP/l cells) adjusted their cellular $Ca^{2+}$ concentration to a lower steady-state value, indicating that the calcium pump was activated by the increase of temperature in the cells supplied sufficiently by ATP. Addition of $CoCl_2$ reduced the $Ca^{2+}$ concentration of fed cells rapidly but did not change the steady-state concentration of cellular calcium in depleted cells (Fig. 2).

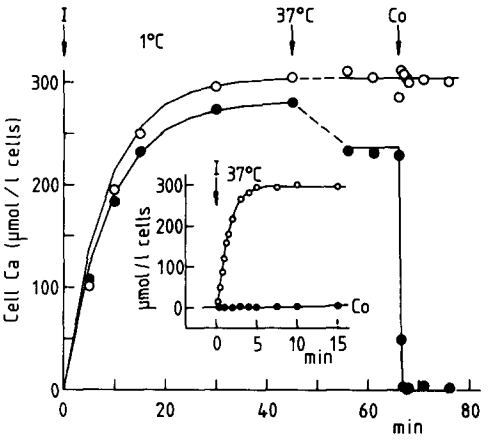


Fig. 2. Effect of cobalt chloride on $Ca^{2+}$ flux. Washed human red cells (glucose-fed or ATP-depleted) were suspended in (mM): NaCl (80), KCl (75), $MgCl_2$ (1), $^{45}CaCl_2$ (0.1), glucose (5) and inosine (6) only in fed cells, pH (37°C) 7.4, cell volume fraction 20%. After equilibration at 1°C ionophore A23187 (50 μmol/l cells) was added at zero time ('I'). At 45 min the suspension was transferred to 37°C (arrow) and after equilibration and sampling $CoCl_2$ was added to a final concentration of 0.25 mM at 66 min ('Co'). The curves were calculated (see mathematical model in Appendix) assuming that the initial A23187-mediated $Ca^{2+}$ influx ($L_{max}$) was (μmol/min per l cells) about 35 at 1°C and 2700 at 37°C before $CoCl_2$ addition, zero after $CoCl_2$ addition. The fed cells were assumed to have a pump flux of zero at 1°C and the calculations gave 420 μmol/min per l cells at 37°C. The depleted cells were assumed to have no pump flux. ●, glucose-fed cells; ○, ATP-depleted cells. Inset: to suspensions of depleted cells (as above) kept at 37°C was added $CoCl_2$ (0.25 mM, ●) or nothing (control, ○) before the addition of A23187 (13 μmol/l cells) at zero time.

These experiments confirm that $CoCl_2$ inhibits the A23187-mediated $Ca^{2+}$ flux, and the agreement between the model curve and the experimental points suggests that there is no major effect on the ATP-dependent $Ca^{2+}$ efflux within 1 min after the $CoCl_2$ addition (cf. above).

In a separate experiment (not shown) the $Ca^{2+}$-ATPase activity of a membrane preparation from human red cells was inhibited approximately 30% by 0.2 mM $CoCl_2$ in the presence of calmodulin. However, in the ATPase experiment the plasma membrane was exposed to $CoCl_2$ for 10–20 min, in contrast to the experiments above in which the A23187-treated cells were exposed to $CoCl_2$ for only a short period of time. This may explain the high $Ca^{2+}$ efflux (360 μmol/min per l

cells) observed during the first 30 s after $CoCl_2$ addition (Fig. 2), which is even 10% higher than the 20 mmol/l cells per hour which is most often referred to as the highest calcium pump activity attainable in experiments with human red cells [1].

*Pump-mediated $Ca^{2+}$ efflux*

By addition of $CoCl_2$ after the addition of A23187 it is possible to block the ionophore-mediated $Ca^{2+}$ flux apparently (see above) with no major effect on the pump-mediated $Ca^{2+}$ efflux, at least for a short period of time. In the experiments below the calcium pump flux was determined during a period of 15 s after $CoCl_2$ addition. By choosing different time intervals between the A23187 addition and the addition of $CoCl_2$ it has been possible to determine the pump flux at different levels of cellular calcium concentration during the ascending ('up') and the descending ('down') phases of a calcium transient.

Such experiments have been performed at three different values of extracellular pH (6.8, 7.1 and 7.4) at the time of A23187 addition. In Figs. 3–5 the calcium pump fluxes are compared with the concentrations of cellular calcium determined at

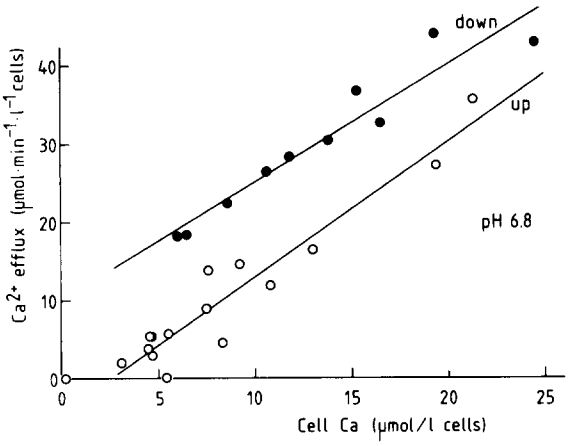


Fig. 3. Pump-mediated $Ca^{2+}$ efflux vs. cellular calcium concentration ($[Ca]_i$) at time of $CoCl_2$ addition. Initial extracellular pH 6.8. Suspensions of human red cells (glucose-fed) were incubated at 37°C in the same medium as in Fig. 1. Twenty-five experiments. The $Ca^{2+}$ influx was initiated by addition of A23187 (11.5 ± 0.3 (S.D.) μmol/l cells). $CoCl_2$ was added to a final concentration of 0.25 mM during either the ascending phase ('up') or the descending phase ('down') of the calcium transient (cf. Fig. 1). $[Ca]_i$ was determined at the time $t$ of $CoCl_2$ addition, at $t + 7.5$ s, and at $t + 15$ s. The pump flux was obtained from these three $[Ca]_i$ values as the slope of a linear regression. The $[Ca]_i$ values were corrected for changes in cellular volume fraction. 'up' phase (○), 'down' phase (●). The 'up' and 'down' curves are regression lines which were significantly different ($P < 0.001$) when tested by Student's $t$ test. Extracellular pH at sampling was (mean ± S.D.) 7.5 ± 0.3 during 'up' phase and 7.4 ± 0.2 during 'down' phase. Intracellular pH (after haemolysis with Triton X-100) was 6.59 ± 0.02.

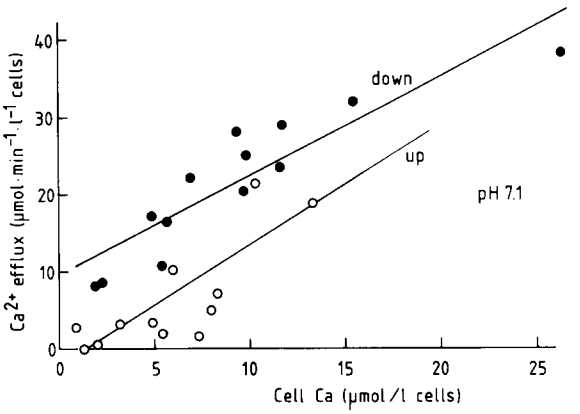


Fig. 4. Same as Fig. 3 but initial extracellular pH 7.1. Twenty-five experiments. A23187 concentration 9.1 ± 0.8 (S.D.). The 'up' and 'down' regression lines are significantly different ($P < 0.001$). Extracellular pH at sampling was (mean ± S.D.) 7.6 ± 0.3 during 'up' phase and 7.8 ± 0.2 during 'down' phase. Intracellular pH was 6.85 ± 0.03.

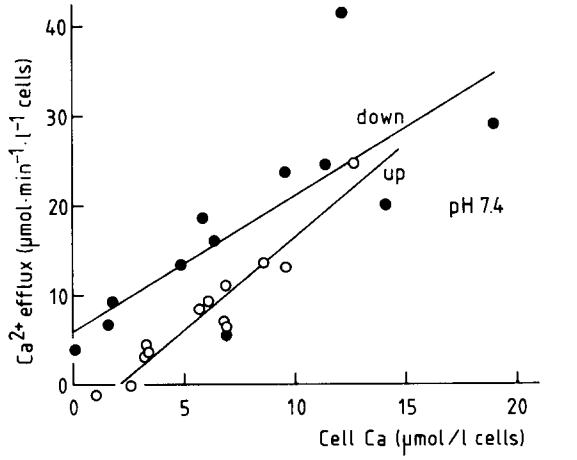


Fig. 5. Same as Fig. 3 but initial extracellular pH 7.4. Twenty-four experiments. A23187 concentration 8.1 ± 0.2 (S.D.). The 'up' and 'down' regression lines are significantly different ($P < 0.02$). Extracellular pH at sampling was (mean ± S.D.) 7.7 ± 0.2 during 'up' phase and 7.7 ± 0.2 during 'down' phase. Intracellular pH was 7.07 ± 0.02.

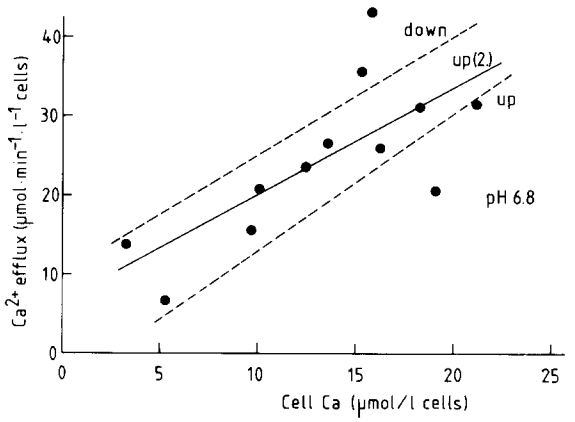


Fig. 6. Same as Fig. 3 but data were from spontaneous second calcium transients from 5 to 20 min after A23187 addition. Only the ascending phase ('up(2.)'). Eight experiments. A23187 concentration 11.5 ± 0.3 (S.D.). For comparison the 'up' and 'down' regression lines from Fig. 3 are shown. The 'up(2.)' regression line is significantly different from both the 'up' curve and the 'down' curve ($P < 0.05$). Extracellular pH at sampling was (mean ± S.D.) 7.3 ± 0.3. Intracellular pH was 6.53 ± 0.03.

the time of $CoCl_2$ addition. Within the measured range of cellular calcium concentrations (up to 25 μmol/l cells of total calcium) the pump flux increased with increasing concentration of cellular calcium, apparently following a linear relationship. However, the data from the 'down' phase of the calcium transients had to be fitted by a regression line which is significantly different from the corresponding regression line fitting the 'up' phase data.

In Fig. 6 the calcium pump fluxes and the corresponding cellular calcium concentrations were obtained from the 'up' phase of spontaneous calcium transients arising subsequent to the primary calcium transients initiated directly by the addition of A23187. In spite of the scattering of the data around the regression line the latter is significantly different from both the 'up' phase and the 'down' phase regression lines obtained from the primary calcium transients.

## Discussion

Figs. 3–5 show that the pump-mediated $Ca^{2+}$ efflux was higher during the descending ('down') than during the ascending ('up') phase of the calcium transient. Provided that equal concentrations of total cell calcium during the 'up' and 'down' phases corresponded to equal concentrations of ionized calcium, the results indicate that the calcium pump responded to a certain $Ca^{2+}$ concentration with a higher pumping rate during the 'down' phase than during the 'up' phase of a transient.

It is not definitely settled whether the calcium pump is electrogenic (for a discussion see Schatzmann [1]). If the pump is electrogenic its activity will depend on the membrane potential, which was reflected by the extracellular pH in our experiments. Therefore, it is important to notice that the extracellular pH values during the 'up' and 'down' phases of the calcium transients were not significantly different (Figs. 3–5).

The validity of attributing cytoplasmic $Ca^{2+}$ values to the total calcium concentration of ionophore-treated human red cells outside equilibrium conditions has recently been questioned [20]. In the present investigation we compared 'up' and 'down' data collected with short intervals (below 2 min), and the investigated cells nearly emptied themselves of calcium after the first transient (Fig. 1), which makes it improbable that any major population of non-pumping calcium-accumulating cells [20] should interfere with our results. However, it is possible that the calmodulin buffering of cytoplasmic $Ca^{2+}$ varied during the calcium transient (see below).

From $Ca^{2+}$-ATPase experiments it is known that the enzyme activity at a given $Ca^{2+}$ concentration depends on the fraction of pump enzyme that binds calmodulin [16,21,22], i.e. the fraction of ATPase in 'B state'.

Analogously, a higher activity of the calcium pump during the 'down' phase can be attributed to a higher fraction of pumps in the calmodulin-binding B state than in the 'up' phase. The reason could be that the pump has been exposed to $Ca^{2+}$/calmodulin for a longer period in the 'down' phase. The 'down' phase data were collected 1.5–2 min after the A23187 addition compared to the 'up' phase data, which were collected 0.25–0.5 min after the start of the experiment.

In order to test this possibility we have simulated the experiments with the aid of the mathe-

matical model described in the Appendix. Fig. 7 shows the results of simulating the experiments carried out at the initial extracellular pH of 7.1. By comparison of Fig. 1 and Fig. 7 (right) it appears that the first transients of extracellular pH and cell calcium concentration are very much alike.

We have simulated the $CoCl_2$ additions by setting the 'A23187-mediated' $Ca^{2+}$ flux equal to zero at various times after the start of the experiment (zero time). The pump-mediated $Ca^{2+}$ efflux was calculated from the resulting $[Ca]_i$ values, just as described in Fig. 3, and the results are shown in Fig. 7 (left). As in Figs. 3–5, the 'down' curve lies above the 'up' curve, and the model predicts that the fraction of calmodulin-binding B state is 1–10% at the sampling time of the 'up' phase (Fig. 7, full curve) but about 85% at the sampling time of the 'down' phase, in agreement with the suggestion above.

The model also predicts that the concentration ratio of cytoplasmic $Ca^{2+}$ to total cell calcium ($\alpha$)

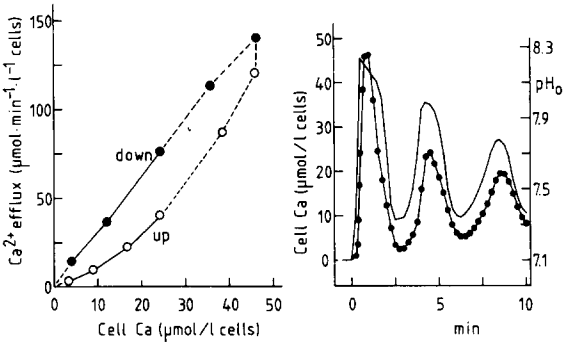


Fig. 7. Simulation of changes in extracellular pH and cellular calcium concentration after A23187 addition (right) and of pump-mediated $Ca^{2+}$ efflux after $CoCl_2$ addition (left). Initial extracellular pH 7.1. Right, A23187 addition at zero time was simulated by increasing net $Ca^{2+}$ influx ($L_x$, see Appendix) from zero to 8.8 μmol/min per l cells. pH (continuous curve), cell Ca (●). Intracellular pH was 6.85. Left, $CoCl_2$ addition was simulated by setting the A23187-mediated $Ca^{2+}$ flux equal to zero ($L_{max} = 0$, see Appendix) at appropriate times during the 'up' phase (○) and 'down' phase (●) of the Ca transient (right). The cell Ca interval identical to that in Fig. 4 is marked by full lines (left). The data were calculated with the aid of the mathematical model described in Appendix. Initial cell volume fraction was 4.2%, $\alpha$ varied between 0.04 and 0.26 during the transients, $S$ was equal to 10 μmol/l cells (Eqn. 5). Maximum pump fluxes were 185 and 295 μmol/min per l cells for 'A-state' and 'B-state' (Eqn. 6).

decreased from about 0.2 to 0.1 during the 'down' phase, i.e. the higher pump fluxes found during the 'down' phase were caused by cytoplasmic $Ca^{2+}$ concentrations which were even lower than those during the 'up' phase. If that is the case in the cells then the hysteretic response is stronger than appears from Figs. 3–5.

The 'up(2.)' curve from the second transient (Fig. 6) is intermediate between the 'up' and 'down' curves from the first transient, and this agrees with the fraction of calmodulin-binding B state that, according to the model, is also intermediate between the fractions during the first transient, viz. 35%.

The 'up' curve in Fig. 7 (left) fits the experimental 'up' curve in Fig. 4. The 'down' curve in Fig. 7, however, is steeper than the corresponding experimental curve in Fig. 4. We do not know the reason for this discrepancy. A comparison of Figs. 3–5 shows that the difference between the 'up' and 'down' curves decreases with increasing initial pH. This is probably due to the lower peak height of the calcium transient at higher pH, especially at pH 7.4, at which the pump activity was maximum, as also found in model calculations. We noticed that transients with reproducible peak height and duration were more difficult to obtain at high pH values.

The model predicts a decrease of cell volume fraction due to the loss of cell water accompanying the KCl efflux caused by the transient opening of the potassium channels. According to the model calculation in Fig. 7 the cell volume fraction (b) decreased 20% during the first transient, compared to the pH 7.1 experiments that revealed a decrease of $22 \pm 2\%$ (S.D., $n = 8$), indicating an adequate choice of parameter values for the model calculations.

In accordance with the experiments (Fig. 1, inset) the model predicts that subsequent to the first pH and calcium transients additional spontaneous transients will occur (Fig. 7, right), i.e. the model predicts oscillations. This is remarkable since the conductance of potassium ions in the model only depends on the concentration of intracellular free $Ca^{2+}$. The potassium channel is assumed to open by binding of two calcium ions, and the calculations suggested that half of the channels were activated at 0.7 μM $Ca^{2+}$. This

apparent $K_d$ is intermediate to those reported previously, ranging from 0.4 $\mu$M (+Mg) [23] to 2–3 $\mu$M [24,25]. The frequency of the transients, however, is higher in the model than in the experiments (Figs. 1 and 7) suggesting that the regulation of the potassium channels may be more complicated (cf. Refs. 18,26–29) than is assumed in our model.

Our experiments support the concept of the calcium pump as part of a hysteretic enzyme system. Taken together the 'up' and 'down' curves in Fig. 7 (left) represent a hysteretic loop, the upper end of the loop corresponding to the top of the calcium transient (Fig. 7, right). The experimental 'up' and 'down' curves (Figs. 3–6) seem to be part of such hysteretic loops.

The hysteresis of the system cannot be assigned to a single component. We have shown (not published) that the only necessary condition for hysteresis in a calmodulin-dependent system is the high affinity of the $Ca^{2+}$-calmodulin complex for the target, e.g. the calcium pump, compared to the low target affinity of calmodulin not complexed by $Ca^{2+}$. The hysteresis manifests itself as delayed activation or deactivation of the system when the concentration of one of the ligands, e.g. $Ca^{2+}$, changes rapidly. This type of hysteresis may be of great importance for the generation and execution of transient signals in other types of cell as well (see also Ref. 30).

## Appendix

The mathematical model used for the simulation of changes in cellular calcium concentration ($[Ca]_i$) and extracellular pH ($pH_0$) is an extension of the model previously described [9,14].

Besides the calculation of A23187-mediated $Ca^{2+}$ net influx, the $Ca^{2+}$/calmodulin-dependent pump-mediated $Ca^{2+}$ efflux, and the degree of calmodulin binding in the cell [9], the extended model includes the calculation of $K^+$ efflux from the cells caused by the opening of the $Ca^{2+}$-sensitive potassium channel. Furthermore the extended model accounts for the hyperpolarisation of the cells due to the opening of the potassium channel, the resulting increase of $pH_0$ in the suspension of the CCCP-treated cells, and the $pH_0$-dependent increase of A23187-mediated net influx of $Ca^{2+}$. Finally, it is assumed in the model that the $K^+$ efflux is accompanied by an equivalent $Cl^-$ efflux and a loss of cell water, leaving the intracellular concentration of KCl unchanged. All other cellular concentrations, however, are corrected for the loss of cell water.

The model calculations imply the solution of four simultaneous differential equations (solved as earlier [9] but using a Digital PDP-11 computer):

$$d[Ca]_i/dt = L - V \tag{1}$$

$$dw/dt = k_1(1-w)Z - k_2 w \tag{2}$$

$$du/dt = k_3(1-u)Z - k_4 u \tag{3}$$

$$d[K]_0/dt = fg_K(E - E_K)/F \tag{4}$$

Eqn. 1 expresses the time dependence of $[Ca]_i$ equal to the A23187-mediated $Ca^{2+}$ net influx ('leak' $L$) minus the pump-mediated $Ca^{2+}$ efflux ($V$):

$$L = (1-\exp(-kt))^{1.5} L_{max}\left(1-(f+\alpha/r^2)[Ca]_i/S\right) \tag{5}$$

$$V = (1-w)v_A + wv_B \tag{6}$$

The first bracket in Eqn. 5 accounts for the time dependence of A23187 uptake in the cell ($k = 7$ $min^{-1}$; for further details see Ref. 14). $L_{max}$ depends on pH according to $\log(L_{max}) = m(pH_0 - pH_x) + \log(L_x)$, $L_x$ being the maximum 'leak' at the initial extracellular pH equal to $pH_x$ and $m$ being a value between 1 and 1.5 dependent on intracellular pH [12] (we chose 1.2 in the pH 7.1 experiments), $f = b/(1-b)$, $b$ being the cell volume fraction, $\alpha$ refers to the concentration ratio of cytoplasmic $[Ca^{2+}]$ to $[Ca]_i$ and depends on the $Ca^{2+}$-buffering effect of calmodulin (see below), $r = \exp(-EF/RT)$, $E$ being the membrane potential and $F$, $R$ and $T$ the Faraday constant, the gas constant, and the absolute temperature, and $S$ is the initial extracellular $Ca^{2+}$ concentration. In Eqn. 6 $v_A$ and $v_B$, the pump activities of the calmodulin-free 'A' state and the calmodulin-saturated 'B' state, are functions of the $Ca^{2+}$ concentration as described earlier [9].

Eqn. 2 defines the time dependence of the fraction $w$ of the calcium pump that binds calmodulin (cf. Eqn. 6), $Z$ being the concentra-

tion of free calmodulin and $k_1$ and $k_2$ being the rate constants for association and dissociation of the pump-calmodulin complex described earlier as functions of the $Ca^{2+}$ concentration [9]. Analogously, Eqn. 3 defines the time dependence of the fraction $u$ of a hypothetical calmodulin target that binds calmodulin and thereby competes with the pump for free calmodulin. The cellular concentrations of calmodulin and calmodulin-binding target were 4 and 3.8 $\mu$M, $k_3 = 13 \cdot k_1$ and $k_4 = 4 \cdot k_2$. Since calmodulin associating to a target binds $Ca^{2+}$ with higher affinity than uncomplexed calmodulin [9], the buffering of cytoplasmic $Ca^{2+}$ depends on $w$ and $u$ and, therefore, $\alpha$ (cf. above) varies during the calcium transient.

Eqn. 4 describes the time dependence of the increment of extracellular $K^+$ concentration due to the opening of the potassium channel. The membrane potential $E$ is equal to $(E_K g_K + E_{An} g_{An})/(g_K + g_{An})$, $E_K$ and $E_{An}$ being the Nernst equilibrium potentials and $g_K$ and $g_{An}$ the conductances of potassium ions and anions, respectively (see Ref. 31). $E_{An}$ and $g_{An}$ are kept constant during the calculations, $E_{An}$ equal to the initial membrane potential (cf. Refs. 32,33). $g_K$ is equal to $g_{Kmax}[Ca^{2+}]^2/(0.5 + [Ca^{2+}]^2)$. $g_{Kmax}$ and $g_{An}$ were 40 and 25 $\mu S/cm^2$ multiplied by $1.75 \cdot 10^7\, cm^2/l$ cells.


## Acknowledgements

We wish to thank Dr. Bent Vestergaard-Bogind for helpful discussions. Expert technical assistance was given by Hanne Jepsen. This work was supported by the Danish Medical Research Council.


## References


1 Schatzmann, H.J. (1985) in Calcium and Cell Physiology (Marme, D., ed.), pp. 18–52, Springer-Verlag, Berlin
2 Al-Jobore, A., Minocherhomjee, A.M., Villalobo, A. and Roufogalis, B.D. (1984) in Erythrocyte Membranes 3: Recent Clinical and Experimental Advances (Kruckeberg, W.C., Eaton, J.W., Aster, J. and Brewer, G.J., eds.), pp. 243–292, Alan R. Liss, New York
3 Larsen, F.L. and Vincenzi, F.F. (1979) Science 204, 306–309
4 Sarkadi, B., Szasz, I. and Gardos, G. (1980) Biochim. Biophys. Acta 598, 326–338
5 Niggli, V., Adunyah, E.S., Penniston, J.T. and Carafoli, E. (1981) J. Biol. Chem. 256, 395–401
6 Macintyre, J.D. and Gunn, R.B. (1981) Biochim. Biophys. Acta 644, 351–362
7 Scharff, O. and Foder, B. (1982) Biochim. Biophys. Acta 691, 133–143
8 Lew, V.L., Tsien, R.Y., Miner, C. and Bookchin, R.M. (1982) Nature 298, 478–481
9 Scharff, O., Foder, B. and Skibsted, U. (1983) Biochim. Biophys. Acta 730, 295–305
10 Ferreira, H.G. and Lew, V.L. (1976) Nature 259, 47–49
11 Vestergaard-Bogind, B. and Bennekou, P. (1982) Biochim. Biophys. Acta 688, 37–44
12 Vestergaard-Bogind, B. and Stampe, P. (1984) Biochim. Biophys. Acta 775, 328–340
13 Tiffert, T., Garcia-Sancho, J. and Lew, V.L. (1984) Biochim. Biophys. Acta 773, 143–156
14 Foder, B., Skibsted, U. and Scharff, O. (1984) Cell Calcium 5, 441–450
15 Lew, V.L. and Brown, A.M. (1979) in Detection and Measurement of Free $Ca^{2+}$ in Cells (Ashley, C.C. and Campbell, A.K., eds.), pp. 423–432, Elsevier, Amsterdam
16 Foder, B. and Scharff, O. (1981) Biochim. Biophys. Acta 49, 367–376
17 Lew, V.L. and Ferreira, H.G. (1978) in Current Topics in Membranes and Transport (Bronner, F. and Kleinzeller, A., eds.), Vol. 10, pp. 217–277, Academic Press, New York
18 Vestergaard-Bogind, B. (1983) Biochim. Biophys. Acta 730, 285–294
19 Sadykov, Y.H., Holmuhamedov, E.L. and Evtodienko, Y.V. (1984) Eur. J. Biochem. 143, 369–371
20 Lew, V.L. and Garcia-Sancho, J. (1985) Cell Calcium 6, 15–23
21 Jarrett, H.W. and Kyte, J. (1979) J. Biol. Chem. 254, 8237–8244
22 Cox, J.A., Comte, M. and Stein, E.A. (1982) Proc. Natl. Acad. Sci. USA 79, 4265–4269
23 Garcia-Sancho, J., Sanchez, A. and Herreros, B. (1982) Nature 296, 744–746
24 Yingst, D.R. and Hoffman, J.F. (1984) J. Gen. Physiol. 83, 19–45
25 Grygorczyk, R., Schwarz, W. and Passow, H. (1984) Biophys. J. 45, 693–698
26 Lew, V.L., Muallem, S. and Seymour, C.A. (1982) Nature 296, 742–744
27 Schwarz, W. and Passow, H. (1983) Annu. Rev. Physiol. 45, 359–374
28 Adorante, J.S. and Macey, R.I. (1986) Am. J. Physiol. 250, C55–C64
29 Alvarez, J., Camaleno, J.M., Garcia-Sancho, J. and Herreros, B. (1986) Biochim. Biophys. Acta 856, 408–411
30 Rasmussen, H. and Barrett, P.Q. (1984) Physiol. Rev. 64, 938–984
31 Vestergaard-Bogind, B., Stampe, P. and Christophersen, P. (1985) J. Membrane Biol. 88, 67–75
32 Knauf, P.A., Fuhrmann, G.F., Rothstein, S. and Rothstein, A. (1977) J. Gen. Physiol. 69, 363–386
33 Bennekou, P. (1984) Biochim. Biophys. Acta 776, 1–9